FUDMA Journal of Sciences (FJS)
ISSN online: 2616-1370
ISSN print: 2645 - 2944
Vol. 7 No. 6, December (Special Issue), 2023, pp 298 -303
DOI: https://doi.org/10.33003/fjs-2023-0706-2193

INVESTIGATION OF PHOTOVOLTAIC POTENTIALS OF A SILVER IMPLANTED DIAMOND-LIKE CARBON THIN FILM

***[1]Abdulsalam, I. G., [1]Abubakar, A. K., [1]Aliyu, M., [2]Naidoo, S. R. and [3]Miller, A.**

[1] Department of Physics, Ahmadu Bello University, Zaria, Nigeria
[2] School of Physics, University of the Witwatersrand, Johannesburg, South Africa
[3] iThemba LABS, Gauteng, Johannesburg, South Africa.

*Corresponding authors' email: abdu.ismaila@gmail.com Phone: +2348174928888
ORCID ID: 0000-0002-3505-6499

ABSTRACT

This paper investigated the optical response of silver implanted carbon-based thin films (deposited on quartz substrates) due to varying fluence of energetic Ag ions in the range 2.5 - 3.4 x 10^{16} ions/cm^2. Raman spectroscopy was used to observe the microstructural specifics of the Ag:a-C composites. Atomic force microscopy (AFM) revealed significant increase in particle grain size and surface roughness of the films at varying fluences. Optical absorption spectra showed that the Surface Plasmon Resonance (SPR) of pristine Ag occurs at visible wavelength of about 428 nm but exhibited a blue shifting (~ 32 nm) in the implanted films. The blue shift in plasmonic wavelength occurs due to the fluence-induced increase in grain size and density of the Ag particles as confirmed by AFM. Optical band gap energy (E_g) and Urbach parameter (E_u) of the pristine carbon film increased, with fluence, from 2.89 eV to 1.60 eV and 3.60 eV to 4.22 eV respectively. The observed optically active parameters strongly indicate that the composites would make good candidates for photon retention towards the enhancement of solar cells' efficiency.

Keywords: amorphous carbon, optical absorbance, surface plasmon resonance, fluence, efficiency

INTRODUCTION

As a unique material, carbon generally exists in two main isotopes (^{12}C and ^{13}C) and is highly unreactive, under normal conditions. Different forms of carbon based materials undergo structural and property modifications when implanted with energetic ions (Karthik et al., 2014). Accelerator-based ion implantation is used to produce shallow surface regions of dopant atoms deposited into appropriate layers of target materials. This process is considered an effective tool for introducing single impurities into the surface layer of a target material to a depth of up to several micrometers (Kroto, 1986). This makes it possible to modify important parameters such as physical, chemical, electrical, mechanical and optical properties of different solid materials (Dai et al., 2012). Ion implantation technique has been employed for various applications in areas like medical (Kumar & Kumar, 2014), optoelectronic (Singhal et al., 2012), photonic devices (Stepanov, 2010), biosensors (Zhou et al., 2009) and photovoltaics (Choi et al., 2008). Several ion species like Ag, Cu, and Au etc. had been implanted on metals, inorganic and polymeric targets for numerous research and industrial purposes (Mak et al., 2012).

This work dwells specifically on the optical response (absorption) of carbon-based thin films irradiated with highly energetic silver ions using accelerator-based ion implantation. Due to obvious interactions with the target atoms, the implanted ions eventually lose their initial projection energy. This energy loss is as a result of collisions with the electrons of the atoms (electronic energy loss) as well as the nuclei of the target atoms (nuclear energy loss) (Laidani et al., 2009). Consequently, several properties of the target material like optical, mechanical and electrical are appreciably altered (modified) depending on the mass, charge and energy of the impinging ions (Mahmudin et al., 2015). For carbon-based nanomaterial, the resultant interaction energy has been established to greatly alter its geometry leading to changes in their dielectric properties and consequently a shift in their surface plasmon resonance (SPR) wavelengths (Candelaria et al., 2012). The SPR wavelength shift in most ion irradiated materials occurs due to the relative change in the orientation and size of the implanted particles (Singhal et al., 2012).

In this work, effort was made to determine the effects of changes in particle size and orientation on the nanomaterials' optical response in relation to the observed SPR wavelength shift.

MATERIALS AND METHODS

Experimental details

Floatable amorphous carbon thin films of thickness 40 µg/cm^2 were obtained for this work. The films were deposited on glass substrates of dimensions 7.5 cm x 2.5 cm and carefully cut into smaller slides of 2.5 cm x 1.5 cm dimensions respectively. Preliminary optical absorption measurement of a reference as-deposited films were carried out on three samples (X, Y and Z) using A Carey UV-visible spectrophotometer. The pristine films were then irradiated with 20 KeV Ag ions delivered by a 350D serial processing ion implantation system at iThemba Labs, Johannesburg, South Africa. Ionic fluence for the three doped samples X, Y and Z were 2.7, 3.0 and 3.3 x 10^{16} ions/cm^2 at an average implantation beam current of 0.55 µA. The electronic (S_e) and nuclear (S_n) energy losses in the carbon matrix for Ag ions at 20 KeV were 2.5 x 10^1 eV/Å and 1.5 x 10^2 eV/Å respectively, and the range of Ag ions in the carbon matrix was ~ 183 Å as determined from SRIM program [31]. Raman spectra were acquired using the 514.5 nm line of a Lexel Model 95 SHG argon ion laser and a Horiba LabRAM HR Raman spectrometer equipped with an Olympus BX41 microscope attachment. The scan range was 100 – 1900 cm^{-1} and the laser power at the sample was approximately 0.4 mW in order to minimize localized heating effects. The Raman analysis was carried out in order to probe the microstructural details of the implanted films. A Veeco Dimension 3100 atomic force microscope was used to study the surface morphology of the films after which onto quartz substrates. Optical absorption measurements were conducted for the film-on-quartz nanocomposites and compared with reference data from the pristine films. Detailed analyses of doping effects of Ag ions on certain optical parameters of the implanted films were later conducted and the results were presented in the next section.

RESULTS AND DISCUSSION

Raman spectroscopy

Raman analysis of a reference carbon film shows similar characteristics with those of microcrystalline graphite showing distinct D and G peaks around 1355 cm^{-1} and 1575 cm^{-1}, respectively as shown in Figure 1(pristine). Other Raman studies of the same material but at different experimental conditions revealed the same trend and referring to the 1355 cm^{-1} mode as the D peak (Freira et al., 1995). The 1573 cm^{-1} line, corresponding to the 1575 cm^{-1} in the work of Tuinstra and Koenig, (1970) is typically referred to as the G peak commonly attributed to Raman active mode of a graphite-like carbon. Ferrari and Robertson, (2004) added that the D peak (1355 cm^{-1}) represents a breathing mode that is only active in carbon films with relative disorder. This shows that the unirradiated film has a clear amorphous phase but with reasonable amount of graphitic micro grains. For the irradiated films, a relative structural disorder was observed such as the growth of D-bands shown in Figure 1(2.7 - 3.4 x 10^{16} ions/cm^{-2}**)** and as summarized by Table. 1. The observed disorder at lower fluence (2.7 - 3.0 x 10^{16} ions/cm^{-2}) is an indication that the Ag nanoparticles are well implanted and that interactions are possible other than the ion-atom interactions within the carbon matrix. At a fluence of 3.3 x 10^{16} ions/cm^{-2}, the micrograph shows particle agglomeration leading to oxide formation as a results of exposure to oxygen atoms in the environment (tarnishing) (Zhang et al., 2019). Hence the observed band, for sample Z, around 240 cm^{-1} is linked to the vibrational modes of Ag in the surface and near surface silver oxide (AgO) phase of the implanted film (Raju et al., 2010).

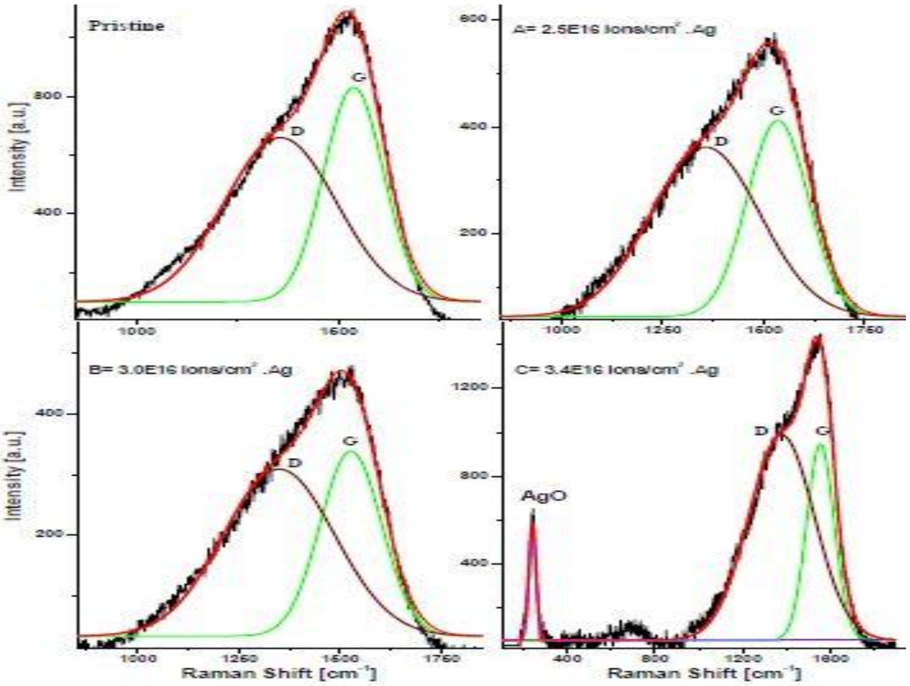

Figure 1: Raman spectra for pristine a-C and Ag:a-C nanocomposites.

Table. 1: Summary of Rama parameters for pristine and Ag irradiated amorphous carbon films.

Samples	G-Peak position (cm^{-1})	I_D (cm^{-1})	I_G (cm^{-1})	I_D/I_G	FWHM(G) (±3.788)	Cluster size, L_a ($\times 10^{-9}$ nm)
Pristine	1575	558.67	731.95	0.763	147.97	5.764
X	1535	317.75	367.56	0.864	151.10	5.090
Y	1544	477.73	492.64	0.970	155.10	4.537
Z	1557	930.12	894.89	1.039	125.93	4.233

Atomic force microscopy

2D AFM micrographs of both pristine and irradiated samples are shown in Fig(a-d). The images revealed that grain size and surface roughness of samples increase as irradiation fluence increases. The surface roughness is attributed to increased sputtering yield due to energetic ion bombardment which affects the smoothness of the pristine sample. The observed increase in average grain size from about 9 nm to about 21 nm is attributed to particle aggregation due to increase in ionic dose from sample A to C respectively.

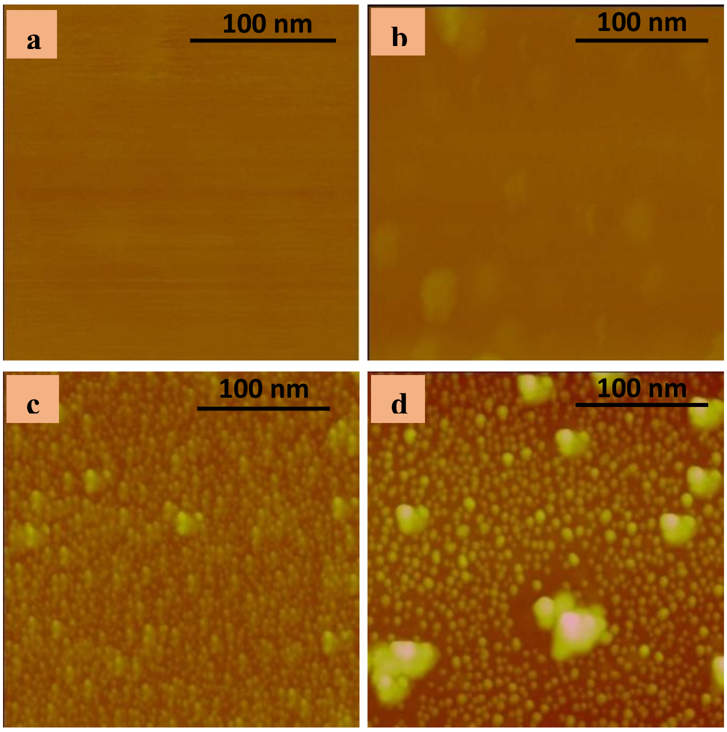

Figure 2: 2D AFM images of (a) pristine a-C and (b(X), c(Y) & d(Z)) Ag:a-C nanocomposites at varying fluences.

UV-visible absorption spectroscopy

Figure Fig 3(a) shows the optical absorption spectrum for pristine carbon film with reasonable transmission in the infrared and near infrared regions of the spectrum (~ 27%) but displayed outright absorption within the visible region. The recorded absorption could be attributed to the density of the film (40 µgcm^{-2}) as well as its inherent antireflection property (Lu & Jiang, 2004). For silver NPs on glass substrate, a clear surface plasmon resonance (SPR) peak was observed at about 427.83 nm as depicted in Fig 3(b). This is in quite a close agreement with the observation, 428 nm, by Lee et al., (2008) Optical spectra for Ag:a-C nanocomposites show proportionate increases in light absorption within the visible and near infrared regions with respect to irradiation fluence until maxima were attained. Fig 3(c) show the combined absorbance spectra of the Ag:a-C nanocomposites analyzed as stand-alone films.

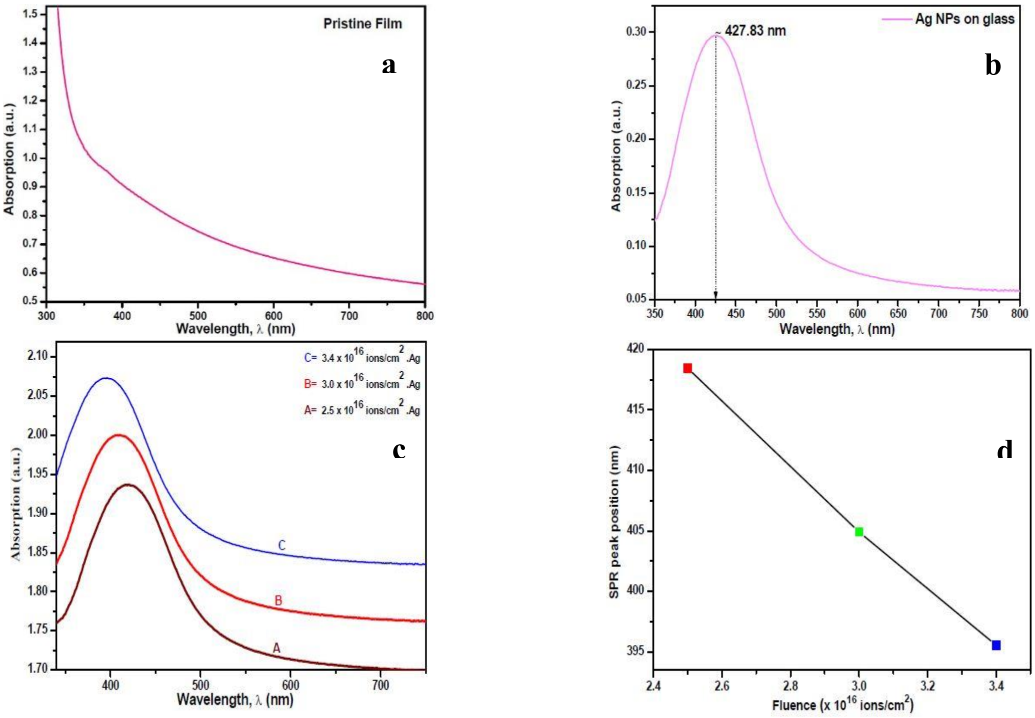

Figure 3: (a, b, c) Optical absorption spectra for pristine a-C, Ag nanoparticles on glass substrate and combined spectra for Ag:a-C nanocomposites. (d) Dependence of SPR peak position on fluence of irradiation.

This rapid absorption increase as well as the clearly observed absorption peaks could be attributed to the surface plasmon resonance (SPR) of Ag nanoparticles embedded in the amorphous carbon matrix. The intense and sharp plasmonic resonance responses of the carbon nanomaterials occur as a result of the variations in the inherent dielectric properties of amorphous carbon leading to small overlaps between the localized SPR of the Ag NPs and their interband transitions that usually start at a wavelength of about 320 nm (Noguez, 2007). Yaremchuk et al., (2014) also suggested that the interaction energy is capable of changing the geometry of the Ag implants leading to a reasonable change in their dielectric properties and consequently the particulate surface plasmon resonance wavelength.

In this work however, particle aggregation is mainly due to low energy (25 keV) and high fluence (~ 10^{16} ions/cm^2) of Ag nanoparticles implying a low accelerator beam current (0.55 μA). As the particles aggregate, their inter-atomic spacing decreases and the distance between two corresponding valence bands reduces thereby increasing the frequency of the electromagnetic emission after being laser-excited and consequently a decreased wavelength (blue shifting) (Eustis & El-Sayed, 2006). Particle size and morphology dependence of the SPR peak positions of Ag nanoparticles have been extensively discussed in some independent but detailed theoretical works on metallic particles' symmetry (González & Noguez, 2007). These works have shown that for uniformly distributed particles, sharply pronounced SPR peaks dominated the optical spectra while broadened peaks with less intensity are prevalent for particles with inconsistent symmetry. Here, the observed dose-influenced SPR peaks for Ag irradiated carbon films are centered within 395.56 nm to 418.46 nm wavelengths for the various implantation doses (Fig 3(c)). The fluence dependence of the SPR peaks and a summary of this dependency are presented in Fig 3(d) and Table 2 respectively.

The optical band gaps of the pristine and irradiated amorphous carbon films were determined using the Tauc's relation given in Eq. (1). According to this relation, the fundamental absorption edge plays central roles in the determination of optical band gap for both direct and indirect interband electronic transitions in the material such the absorption coefficient (α) as a function of photon energy ($h\upsilon$) is given by (Tauc et al., 1966).

$$(\alpha h\upsilon)^{\frac{1}{r}} = A\left(h\upsilon - E_g\right) \qquad (1)$$

where A is a constant, $h\upsilon$ defines the photon energy in electron-volt (eV), E_g is the optical band gap energy of the material which represents the energy difference between the valence and conduction bands, respectively, while r is an index having values between $\frac{1}{2}$ and 3 depending on the nature of the interband electronic transitions. A plot of $(\alpha h\upsilon)^{\frac{1}{r}}$ versus $h\upsilon$ yields a curve whose extrapolation in the linear portion to the $h\upsilon$ axis (i.e. $\alpha = 0$) gives the optical band gap energy.

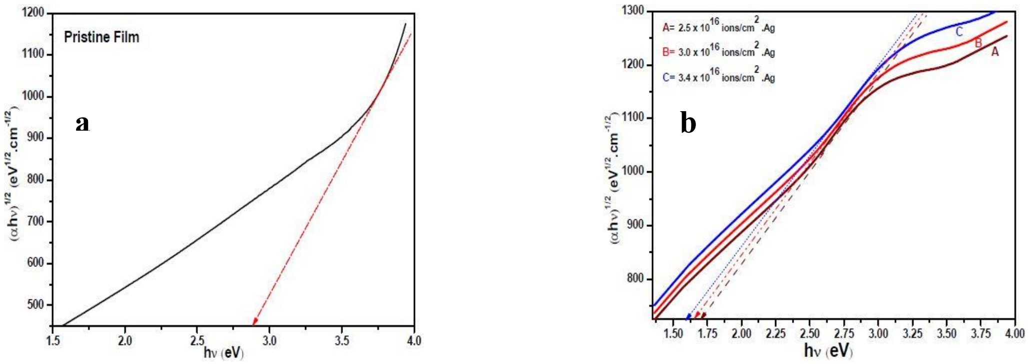

Figure 4: Tauc plots for (a) Pristine and (b) combined Ag:a-C nanocomposites showing respective optical bang gap energies.

The Tauc plots in Fig. 4 show significant decrease in the optical gap of the films from 2.89 eV for pristine a-C to 1.60 eV for the lowest fluence nanocomposite. A similar trend (i.e. red shifting of optical band gap) has been previously reported (Ahmed et al., 2009) for sp^3-rich diamond-like amorphous carbon films doped with varying concentrations of Ag nanoparticles during deposition; optical bang gap decreased from 2.55 eV to 1.95 eV. The observed decrease in optical band gaps of these nanocomposites can be attributed to absorption by the Ag NPs and the effect of their increased doses in the amorphous carbon as previously suggested by Ahmed et al., (2008).

One of the standards used as a yardstick in measuring inhomogeneous disorder in amorphous systems is the Urbach energy, E_u. Due to the prevalence of short order ranges in amorphous systems, the valence and conduction bands are not characterized by sharp optical absorption edges but tails of localized states which are extended in the band gap (Shaheen et al., 2011). Hence, the absorption coefficient is related to the Urbach parameter (Urbach, 1953) as follows;

$$\ln \alpha = \frac{1}{E_u} h\upsilon + \ln \alpha_0 \qquad (2)$$

A plot of $\ln \alpha$ versus photon energy ($h\upsilon$) in Eq. (2) was used to determine the Urbach energy, E_u of the nanocomposite by evaluating the inverse of each slope along the linear portions of the respective curves.

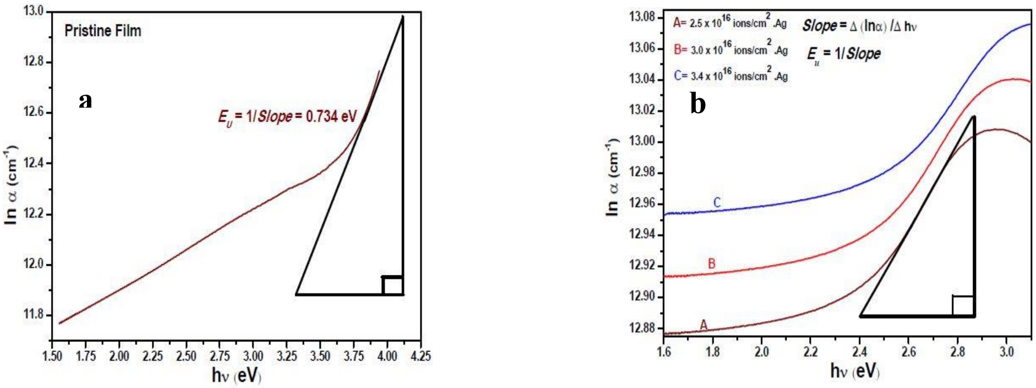

Figure 5: Urbach plots for (a) Pristine a-C and (b) Ag:a-C nanocomposites showing respective Urbach parameters.

Figure 5(a & b) show the Urbach plots for pristine and Ag irradiated a-C films. Respective values of E_u were observed to increase in proportion to increasing fluence of Ag NPs; from 3.60 eV for pristine film to 4.22 eV for nanocomposite with highest irradiation dose. Increase in E_u values, which demonstrated great usefulness in probing disorder (Patsalas, 2011), is attributed to cluster size distribution that helps in evaluating the optical response (particularly absorption) due to defect states in amorphous carbon nanostructures (Robertson, 2002). The stronger the interaction, the higher the Urbach energy values and more bands' bending leading to reductions in optical band gap. In order words, increasing fluence of Ag nanoparticles increases the Urbach energy and, by extension, reduces the optical band gap energy (Naidoo & Ismaila, 2019; Ismaila et al., 2019).

Table 2: Summary of major optical parameters for pristine a-C and the respective Ag:a-C films

Optical parameters	**Pristine film**	**X**	**Y**	**Z**
Optical band gap energy, E_g (eV) (±0.03)	2.89	1.71	1.65	1.60
Urbach energy, E_u (eV) (±0.2)	3.60	3.89	3.90	4.22
SPR Peak position, (nm)	-	418.46	404.92	395.56

CONCLUSION

In this paper, optical characterization of Ag implanted Diamond-like-carbon (DLC) thin films was conducted. The silver incorporation has induced substitutional defects which distorted the inherent electronic structure of the DLC thereby leading to changes in the overall optical transparency and optical band gap. Optical band gap decreases from 2.89 eV to 1.60 eV while Urbach energy increases from 3.60 eV to 4.22 eV. A potential advantage of this tunable band gap can be taken by adequate control of nanoparticle doping for advanced nanoscale materials research and for optimization of applications in such areas as surface coatings and as functional materials for solar cell efficiency enhancement.

Acknowledgements

This work has been supported financially by the Tertiary Education Trust Fund (TETFUND) Institution Based Research Project Grant No: TETF/DR&D/UNI/ZARIA/IBR/2020/VOL.1/40. The authors would also like to thank Mr. A. Miller of iThemba LABS, Gauteng, South Africa for facilitating the ion implantation session and the Microscopy and Microanalysis Unit (MMU), Wits University, South Africa for facilitating the UV-Visible and AFM sessions.

REFERENCES

P. S. Karthik, A. L. Himaja, and S. P. Singh, "Carbon-allotropes: synthesis methods, applications and future perspectives," *Carbon Lett.*, vol. 15, no. 4, pp. 219–237, 2014.

H. Kroto, "Space, Stars, C_{60}, and Soot," *Science* (80-.)., vol. 242, no. 4882, pp. 1139–1145, 1986.

L. Dai, D. W. Chang, J. B. Baek, and W. Lu, "Carbon nanomaterials for advanced energy conversion and storage," *Small*, vol. 8, no. 8, pp. 1130–66, 2012.

P. Kumar and A. Kumar, "Carrier type modulation in current annealed graphene layers," *Appl. Phys. Lett.*, vol. 104, no. 8, 2014.

R. Singhal, J. C. Pivin, R. Chandra, and D. K. Avasthi, "Ion irradiation studies of silver/amorphous carbon nanocomposite thin film," *Surf. Coatings Technol.*, vol. 229, pp. 50–54, 2013.

A. L. Stepanov, "Synthesis of silver nanoparticles in dielectric matrix by ion implantation: A review," *Rev. Adv. Mater. Sci.*, vol. 26, no. 1–2, pp. 1–29, 2010.

L. H. Zhou et al., "Formation of Au nanoparticles in sapphire by using Ar ion implantation and thermal annealing," *Nucl. Instruments Methods Phys. Res. Sect. B Beam Interact. with Mater. Atoms*, vol. 267, no. 1, pp. 58–62, 2009.

H. W. Choi, R. H. Dauskardt, S. C. Lee, K. R. Lee, and K. H. Oh, "Characteristic of silver doped DLC films on surface properties and protein adsorption," *Diam. Relat. Mater.* vol. 17, no. 3, pp. 252–257, 2008.

K. F. Mak, L. Ju, F. Wang, and T. F. Heinz, "Optical spectroscopy of graphene: From the far infrared to the ultraviolet," *Solid State Commun.*, vol. 152, no. 15, pp. 1341–1349, 2012.

N. Laidani, R. Bartali, G. Gottardi, M. Anderle, and P. Cheyssac, "Optical absorption parameters of amorphous carbon films from Forouhi – Bloomer and Tauc – Lorentz models : a comparative study," *J. Phys. Condens. Matter, IOP Publ.*, vol. 20, no. 1, p. 015216,1-015216,8., 2009.

L. Mahmudin, E. Suharyadi, A. Bambang, S. Utomo, and K. Abraha, "Optical Properties of Silver Nanoparticles for Surface Plasmon Resonance (SPR) -Based Biosensor Applications," no. July, pp. 1071–1076, 2015.

S. L. Candelaria et al., "Nanostructured carbon for energy storage and conversion," *Nano Energy*, vol. 1, no. 2, pp. 195–220, 2012.

F. L. Freire, C. A. Achete, and G. Mariotto, "Nitrogen implantation into amorphous carbon films: XPS, AES and Raman analyses," *Nucl. Inst. Methods Phys. Res. B*, vol. 99, no. 1–4, pp. 606–609, 1995.

F. Tuinstra and J. L. Koenig, "Raman Spectrum of Graphite," *J. Chem. Phys.*, vol. 153, no. 3, pp. 1126–1130, 1970.

A. C. Ferrari and J. Robertson, "Raman spectroscopy of amorphous, nanostructured, diamond-like carbon, and nano-diamond," *Philos. Trans. R. Soc. A Math. Phys. Eng. Sci.*, vol. 362, no. 1824, pp. 2477–2512, 2004.

D. Zhang, P. Yi, L. Peng, X. Lai, and J. Pu, "Amorphous carbon films doped with silver and chromium to achieve ultra-low interfacial electrical resistance and long-term durability in the application of proton exchange membrane fuel cells," *Carbon N. Y.*, vol. 145, pp. 333–344, 2019.

N. R. C. Raju, K. J. Kumar, and A. Subrahmanyam, "Silver oxide (AgO) thin films for Surface Enhanced Raman Scattering (SERS) studies," *AIP Conf. Proc.*, vol. 1267, pp. 1005–1006, 2010.

H. M. Lu and Q. Jiang, "Size-Dependent Surface Energies of Nanocrystals," *J. Phys. Chem. B*, vol. 108, no. 18, pp. 5617–5619, 2004.

K. C. Lee, S. J. Lin, C. H. Lin, C. S. Tsai, and Y. J. Lu, "Size effect of Ag nanoparticles on surface plasmon resonance," *Surf. Coatings Technol.*, vol. 202, no. 22–23, pp. 5339–5342, 2008.

C. Noguez, "Surface plasmons on metal nanoparticles: The influence of shape and physical environment," *J.Phys. Chem. C*, vol. 111, no. 10, pp. 3606–3619, 2007.

I. Yaremchuk, A. Tamulevičiene, T. Tamulevičius, K. Šlapikas, Z. Balevičius, and S. Tamulevičius, "Modeling of the plasmonic properties of DLC-Ag nanocomposite films," *Phys. Status Solidi Appl. Mater. Sci.*, vol. 211, no. 2, pp. 329–335, 2014.

S. Eustis and M. A. El-Sayed, "Why gold nanoparticles are more precious than pretty gold: Noble metal surface plasmon resonance and its enhancement of the radiative and non-radiative properties of nanocrystals of different shapes," *Chem. Soc. Rev.*, vol. 35, no. 3, pp. 209–217, 2006.

A. L. González and C. Noguez, "Influence of Morphology on the Optical Properties of Metal Nanoparticles," *J. Comput. Theor. Nanosci.*, vol. 4, no. 7–8, pp. 1249–1252, 2007.

A. Tauc, J., Grigorovici, R., Vancu, "Optical properties and electronic structures of amorphous germanium," *Phys. Stat. Sol.*, vol. 15. pp. 627–637, 1966.

S. F. Ahmed, M. W. Moon, and K. R. Lee, "Effect of silver doping on optical property of diamond like carbon films," *Thin Solid Films*, vol. 517, no. 14, pp. 4035–4038, 2009.

S. F. Ahmed, M. W. Moon, and K. R. Lee, "Enhancement of electron field emission property with silver incorporation into diamond-like carbon matrix," *Appl. Phys. Lett.*, vol. 92, no. 19, pp. 1–4, 2008.

A. Shaheen, W. Zia, A. Khalid, and M. S. Anwar, "Band Structure and Electrical Conductivity in Semiconductors," *Mater. Eng.*, pp. 1–26, 2011.

F. Urbach, "The Long-Wavelength Edge of Photographic Sensitivity and of the Electronic Absorption of Solids," *Phys. Rev.*, vol. 92, no. 5, pp. 1324–1324, 1953.

P. Patsalas, "Optical properties of amorphous carbons and their applications and perspectives in photonics," *Thin Solid Films*, vol. 519, no. 12, pp. 3990–3996, 2011.

J. Robertson, "Diamond-like amorphous carbon," *Mater. Sci. Eng. Reports*, vol. 37, no. 4–6, pp. 129–281, 2002.

A. Ismaila, T.O. Ahmed, and H. Ismail: (2019) "Variational Effects of TiO_2 Doping on Optical Response of Polymer Blend Nanocomposites". *FUDMA Journal of Sciences (FJS)*, 3(3): pp. 377-380.

S. R. Naidoo & A. Ismaila: (2019) "Fluence Enhanced Optical Response of Ag Implanted Carbon Thin Films". *Journal of Carbon Research (C)*, 5(45): pp. 1-12. doi:10.3390/c5030045